Geomechanics and Engineering, *Vol. 26, No. 4 (2021) 385-399*
https://doi.org/10.12989/gae.2021.26.4.385

Dynamic response of CFG and cement-soil pile composite foundation in the operation stage

Xuansheng Cheng*[1,2], Jianchao Chen[2], Xiangdong Cai[1,2], Xiaoyan Zhang[1,2], Lijun Gong[1,2] and Chengyue Gu[3]

[1]*Western Engineering Research Center of Disaster Mitigation in Civil Engineering of Ministry of Education, Lanzhou University of Technology, Lanzhou, 730050, PR China*
[2]*School of Civil Engineering, Lanzhou University of Technology, Lanzhou, 730050, PR China*
[3]*China Railway 21st Bureau Group Sixth Engineering Co., LTD., Lanzhou, 730070, PR China*

(Received December 4, 2019, Revised July 7, 2021, Accepted August 6, 2021)

Abstract. More and more attention is paid to the stability, safety and comfort of trains during its operation stage. When the train is running, in addition to the track gravity, it is also affected by the train load and earthquake, these dynamic effects will have a certain impact on the normal operation of the railway. However, the current research on the dynamic response of composite CFG and cement-soil compaction piles foundations under dynamic loads is rarely involved. Taking the composite foundation of Baoji-Lanzhou Passenger Dedicated Line as the research object, the dynamic response of the composite foundation under train load, seismic wave and train-seismic load is analyzed in detail by using numerical simulation software. The results show that under the train load, the maximum displacement occurs at the action position of the train load, and it is gradually reduced downward. The overall displacement is not large, and the influence on the operation of the train is little. Under earthquake action, the displacement is the largest at the bottom of subgrade, and gradually decreases upward, which has little effect on the top of embankment. Under the train-earthquake action, the displacement of subgrade bottom and embankment top is larger, and gradually decreases to the middle. It provides the corresponding theoretical basis for the same type of railway subgrade engineering.

Keywords: CFG and cement-soil compaction pile; composite foundation; dynamic response; numerical simulation; seismic wave

1. Introduction

With the rapid development of China's national economy, the highspeed railway has developed rapidly. Because of its long operation period and fast train speed, the requirements for settlement control are much stricter than those for ordinary railway. In collapsible loess area, CFG and cement-soil compaction pile composite foundation is a long short pile composite foundation and it begin to be applied in this area. CFG and cement-soil compaction pile composite foundation has fully played the role of two kinds of piles: the CFG pile has long length and large rigidity, which can transfer the upper load to a deeper soil layer and greatly improve the bearing capacity of the composite foundation; the cement-soil compaction pile spacing is small, the arrangement is relatively dense, which can effectively eliminate the collapse of the upper loess. Although CFG pile and cement soil compaction pile composite foundation has been applied, due to its complex working mechanism under the action of train load, the research on this kind of foundation is not enough at present.

Many scholars have studied the dynamic load of the train. Milnen *et al.* (2017) analyzed the spectral characteristics of train dynamic loads by monitoring the load of railway trains. Germonpre *et al.* (2018) studied the influence of longitudinal roughness and stiffness on railway vibration from the point of view of track. In China, Sun *et al.* (2017) used the time history calculation of the measured rail vibration acceleration to get the simulated subway train load. Nie *et al.* (2017) systematically tested the dynamic displacement, acceleration and dynamic strain of piers caused by different speeds and vehicles types at different parts of the piers, and obtained the dynamic load parameters of bridge foundations with different spans.

CFG pile and cement soil compaction pile composite foundation is a kind of composite foundation with composite piles. According to the characteristics of pile, CFG pile is selected as long pile and cement soil compaction pile as short pile. CFG pile is a high cohesive strength pile formed by cement, fly ash, sand gravel, gravel, sand stone and appropriate amount of water, which forms a composite foundation together with the soil between pile and cushion. Nowadays, there are more and more analytical, experimental and numerical methods to study composite foundation. In terms of theoretical analysis, Castro and Sagaseta (2009) gave an analytical solution for the consolidation of composite foundations considering the lateral deformation of stone columns. Cheng *et al.* (2017)

*Corresponding author, Professor, Ph.D.
E-mail: chengxuansheng@gmail.com; chengxslut@sina.com

ISSN: 2005-307X (Print), 2092-6219 (Online)

proposed two simplified composite ground treatment methods. Leung *et al.* (2017) combined the bending characteristics of pile groups and pile raft foundation superstructures, using the cohesion matrix, combining the stiffness of the superstructure with the foundation model, an analysis and optimization method for pile groups and pile raft foundations is proposed. Handy (2001) found that high side pressure will affect the load value of the foundation, and high side pressure will increase the load value of the foundation. Smadi (2001) found that the maximum lateral displacement of the toe end of a stable embankment is approximately equal to the total settlement during the construction process, which is about 20% of the total settlement after construction. Loganathan *et al.* (1993) found that the maximum lateral displacement under the load of the embankment was 0.28 times the maximum settlement of the embankment center.

In order to study the performance of composite foundation, many researchers have carried out experimental research. Lai *et al.* (2016) used finite element method and laboratory model test to study the settlement behavior of soft soil foundation of saturated tailings dam under the treatment of CFG pile composite foundation. It was found that CFG pile treatment can effectively strengthen the saturated tailings dam, and the load has little impact on the settlement of the soil between piles. The settlement of FEM in the change of soil between piles is in good agreement with the laboratory model test. Wang *et al.* (2018) simulated pile raft composite foundation and pile geogrid composite foundation with different pile spacing through centrifugal model test to study the time effect of negative friction of rigid piles in high-speed railway. Xue *et al.* (2019) based on the large-scale X-section pile network composite foundation model, the dynamic characteristics of pile network composite foundation under the train load of high-speed railway are studied. The distribution characteristics of dynamic stress, dynamic displacement, velocity and acceleration of subgrade soil under different train speeds are analyzed; the vibration response of track subgrade system under cyclic subgrade load and the distribution characteristics and attenuation laws of dynamic stress inside subgrade are studied. Faro *et al.* (2015) conducted a series of horizontal load pile tests in natural foundation and cement soil, and finally obtained that after cement soil treatment, the lateral resistance of short pile increased significantly. Sales *et al.* (2017) conducted a test procedure in a large calibration room for the installation of single pile and pile group in three sand samples of different densities, and evaluated the tests of no pile and driven pile to evaluate the impact of pile installation process on pile load settlement response. Finally, a prediction method of pile group load settlement response based on single pile response is proposed. Moayed *et al.* (2013) used the finite element method to study the bearing capacity of this kind of foundation under the vertical load. Based on the study of different pile placement methods under different vertical stress levels, the optimal pile placement method with minimum settlement was determined. It was found that the arrangement effect of long and short piles was more obvious with the increase of raft vertical stress. In addition,

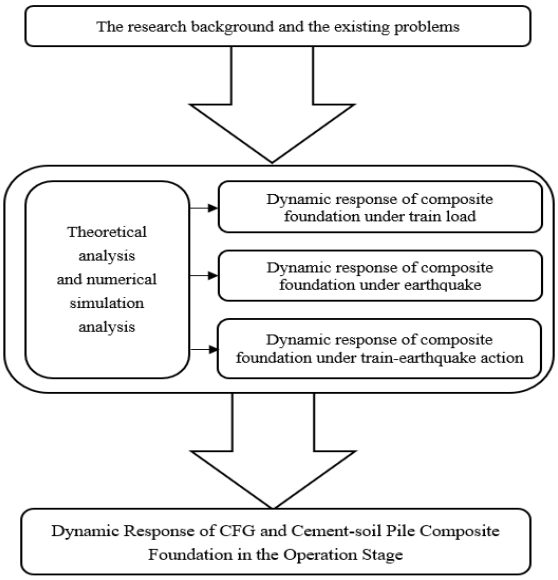

Fig. 1 The flowchart of research steps of the text

a new factor named "composite pile raft efficiency" (CPRE) is defined, which determined the arrangement efficiency of long and short piles in composite pile raft foundation. In addition, it was found that the settlement changes of different long and short piles were in good agreement with the changes of CPRE ratio. Through experiments and discrete element methods (DEM), the mechanical characteristics of high-speed railway subgrades are explored, and the change law of ballast degradation is also analyzed (Zhang and Gao, 2020; Zhang et al, 2020).

Discrete element method (DEM) is a numerical simulation method specially used to solve the problem of discontinuous media. It can simulate the nonlinear large deformation characteristics of jointed rock masses more realistically. Finite element method is to discretize the complex geometric area of the medium into elements with simple geometric shapes. Finite and interrelated elements can be used to simulate an infinite complex body, thereby modeling, analyzing and calculating results. For linear elastic problems, a convergent solution can be obtained when the actual structure displacement field function is continuous and smooth. When studying the dynamic response law of the combined dynamic load of CFG+ cement-soil compacted pile subgrade, the loess is continuous material, the method of subdividing the elements of the finite element method obtains a sufficiently approximate simulation, which makes the calculation result more accurate, faster calculation speed, and the application has accumulated a wealth of experience in long-term large-scale engineering. Therefore, finite element method is used in this paper.

In this paper, according to the working conditions of CFG pile and cement-soil compaction pile composite foundation, and the construction standards of high-speed railway, combined with the situation of Baolan line, the dynamic response of CFG pile and cement soil compaction pile composite foundation system under train load, seismic wave, train-seismic load is simulated, the settlement and

stress characteristics of composite foundation is also studied, aiming to provide some refences for similar cases in the future. The flowchart of the main research steps and methods are shown in Fig.1.

2. Dynamic response of a CFG and cement-soil compaction pile composite foundation under a train load

2.1 Train track force simplification

The train load is a very complex dynamic load (Zhang *et al.* 2001). While considering the axle load and suspension system of the train, the external environment of the train, such as the composition of the track and the irregularity should also be taken into account. In the finite element analysis, the train track force needs to be simplified. The initial simplified method is to convert the train load into soil column and calculate it by static load. In recent years, the train has been accelerated many times, and the simple static conversion method has been unable to meet the engineering requirements. During the train running, the vibration load is diffused in the form of Rayleigh wave. The field measured data of train load can provide the basis for the study, but the field monitoring data are very limited, so the finite element simulation method can be used for analysis.

The existing simulation methods of train track force are as followings:

(1) Vehicle-track space coupling dynamics model

The vehicle-track spatial coupling dynamic model is a relatively perfect dynamic model, considering the nonlinearity of wheel-rail contact and the irregularity of track, and the track force of the train is obtained through the calculation program. However, this method has a large amount of calculation, which is not applicable to the general train dynamic analysis problem, so it is necessary to further simplify the vehicle and track models.

(2) Simple vertical vibration model of train

If the horizontal vibration caused by the contact between the train and the track is ignored, only the vertical vibration is considered, and it is considered that the train and the track are bound to each other, the train model can be simplified as follows:

In the coordinate system of Fig. 2, a differential equation for the vertical motion equilibrium of the wheel and rail can be obtained:

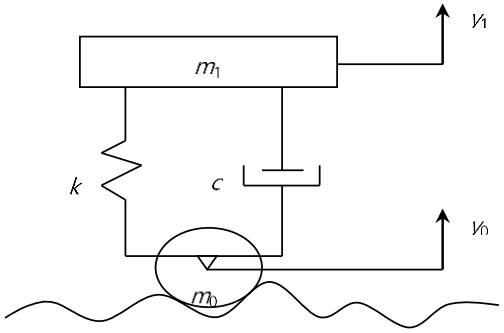

Fig. 2 Simplified model of train

$$m_2\left(\ddot{y}_1-\ddot{y}_0\right)+c\left(\dot{y}_1-\dot{y}_0\right)+k\left(y_1-y_0\right)=0 \tag{1}$$

Setting the absolute displacement y_r=y_1-y_0, Eq. (1) can be expressed as:

$$m_2\ddot{y}_r+c\dot{y}_r+ky_r=0 \tag{2}$$

The interaction forces between tracks P(t) can be obtained by the Daramber principle:

$$\begin{aligned}P(t)&=(m_1+m_2)g+m_2\ddot{y}_1+m_1\ddot{y}_0=\\&(m_1+m_2)g+(m_1+m_2)\ddot{y}_0+m_2\ddot{y}_r\end{aligned} \tag{3}$$

(3) Artificial numerical excitation method

On the basis of experimental and theoretical studies, considering the requirements of track irregularity, the British Railway Technology Center proposed that the dynamic load of trains can be simulated by an exciting force function containing static load and a series of sine functions (Zhang et al, 2001)

$$P_t=P_0+P_1\sin\omega_1t+P_2\sin\omega_2t+P_3\sin\omega_3t \tag{4}$$

In the formula, P_0 is the static load of the wheel, P_1 is a typical vibration load corresponding to the driving smoothness control condition, P_2 is a typical vibration load corresponding to the dynamic additional load control conditions on the line, and P_3 is a typical vibration load under the condition of waveform wear control.

If the mass of a train under a spring is M_0, then the corresponding vibration load amplitude is:

$$P_i=M_0a_i\omega_i^2\left(i=1,2,3\right) \tag{5}$$

where, a_i is corresponding to a typical vector height with control standards I, II and III in Table 1, and ω_i is the circular frequency at the irregular vibration wavelength under the corresponding control standards I, II and III at the corresponding vehicle speeds. The formula for calculating the circular frequency is:

$$\omega_i=2\pi v/L_i \tag{6}$$

where, v is the running speed of the train, L_i is a typical wavelength corresponding to the three control standards I, II, and III.

Table 1 Wavelength and Vector Height of Irregular Vibration in Train Load Simulation

Control condition	Wavelength L_i/m	Version/mm
According to driving smoothness (I)	50.0	16.0
	20.0	9.0
	10.0	5.0
According to the dynamic additional load acting on the line (II)	5.0	2.5
	2.0	0.6
	1.0	0.3
Waveform wear (III)	0.5	0.1
	0.05	0.005

Table 2 Material parameters

Material	Modulus of elasticity (MPa)	Poisson's ratio	Density (kg/m^3)	Internal friction angle (°)	Cohesion (kPa)
Mattress layer	50	0.25	2000	15	30
Soil	10	0.35	1800	10	15
CFG pile	20000	0.25	2500	-	-
Cement-soil compacted pile	2000	0.28	2000	-	-

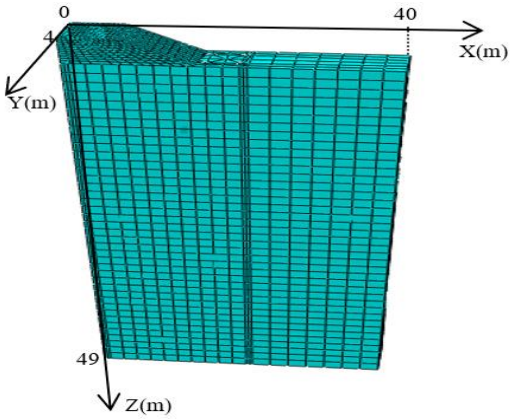

Fig. 3 Schematic diagram of grid division/m

When the corresponding train parameters and irregularity control standards are determined, the wheel-rail force can be calculated by the Eq. (4) to (6). This method comprehensively considers the factors of train, train speed and track irregularity, and can reasonably simulate the wheel-rail force of trains.

2.2 Dynamic response of CFG and cement-soil compaction pile composite foundation

2.2.1 Selection of composite foundation parameters

This section selects CFG-cement soil compaction pile composite foundation for dynamic analysis under train load. The CFG pile diameter is 400 mm, the pile spacing is 1.6m, and the pile length is 22 m. The cement-soil compaction pile length is 9 m, the pile diameter is 400 mm, the pile spacing is 0.9 m and the thickness of the cushion layer is 500 mm. According to on-site railway foundation design parameters and survey data, the physical parameters of the material are obtained, as shown in Table 2. (Note: The main component of the subgrade foundation geology is loess, because of the collapsibility of loess, CFG-cement-soil compaction pile composite foundation is adopted. CFG pile belongs to rigid pile, and its main function is to enhance the bearing capacity of foundation. Cement soil compaction pile belongs to flexible pile, the main function is to dismiss the collapsibility of loess. Combined with relevant engineering cases and field actual data, the elastic modulus of CFG pile is 10 times higher than that of cement-soil compaction pile in the selection process of modeling parameters.).

The actual width of the bottom of the composite foundation is 32 m, and the calculated width of the foundation is 2.5 times the width of the bottom of the composite foundation, which is 80m; considering the impacted depth of the additional stress and settlement deformation of the pile, the calculated depth of the foundation is 2 times the longest pile length, which is 44m; the filling height of the embankment is 5m. Because the maximum pile spacing is 1.6 m, the calculated length should be greater than twice the pile spacing, which is taken as 4 m. The finite element model of CFG and cement-soil compaction pile composite foundation is established, and the model is meshed. When meshing, considering the stiffness difference between master and slave surfaces, the grid density of slave surfaces is larger than that of master surfaces. In order to facilitate calculation, the grid density of the pile-free part of the subgrade can be appropriately increased. At the same time, in order to improve the calculation accuracy, the grid density of soil between piles should be relatively fine, and the grid division is shown in Fig. 3 (Because the model is symmetrical, only half of it is chose for analysis).

Boundary conditions: In order to avoid reflection of seismic waves on the boundary, it is necessary to introduce an artificial boundary, a viscous boundary is used in the model, namely, a damper is added to the soil boundary to form a viscous boundary. It can be realized through the selection: "Springs/Dashpots" in "Special" of the "Interaction" part. Then define the load and boundary conditions in the "Load" part, and apply gravity to the entire model in the "Geostatic" analysis step. In the "Dynamic" analysis step, the vertical displacement of the model bottom is fixed, and the lateral displacement (normal displacement) of the surrounding boundary of the model is fixed.

2.2.2 Train load selection

The selection of train load is very important when simulating train load. When using finite element method to simulate train load, there are usually three methods (Niu *et al.* 2018): moving static load method, artificial excitation method and time history boundary method.

Moving static load method is mainly divided into the following two steps: to determine the size and location of the wheelset static load by the axle load and wheelset distribution of a specific vehicle. This series of loads react on the subgrade surface and move along the subgrade surface according to a certain speed.

The artificial excitation method is mainly divided into the following two steps: the periodic train load is artificially established according to the vibration frequency domain characteristics of the subgrade, and the train load corresponds to the high energy frequency band generated by the wheel eccentricity, the track face smoothness, and the wheel spacing. The corresponding parameters are adjusted according to different vehicle types and vehicle speeds and applied to the subgrade surface.

Time history boundary method is mainly divided into the following two steps: take the train through the measured subgrade surface velocity, acceleration, stress, displacement and other load time history parameters as the standard to establish a model consistent with the actual model. The corresponding velocity boundary, acceleration boundary,

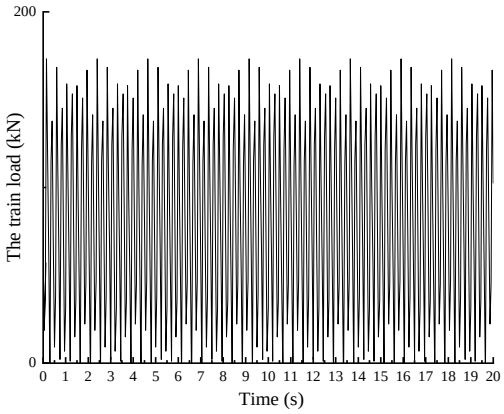

Fig. 4 Train load simulation time history curve

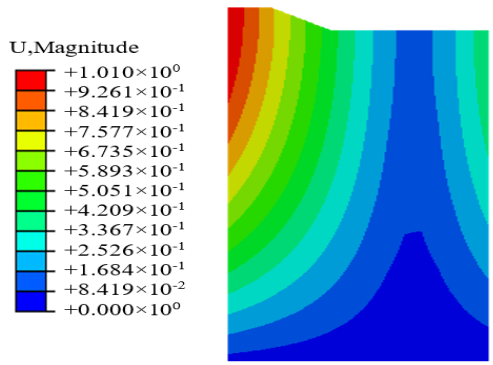

(a) First-order mode

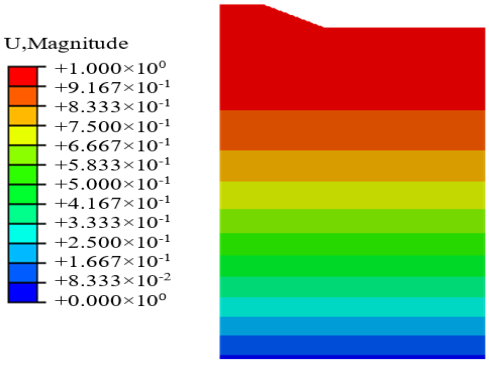

(b) Second-order mode

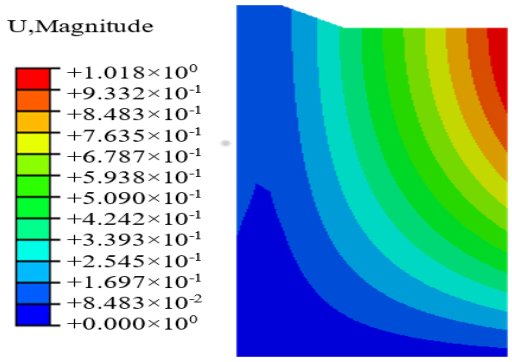

(c) Third-order mode

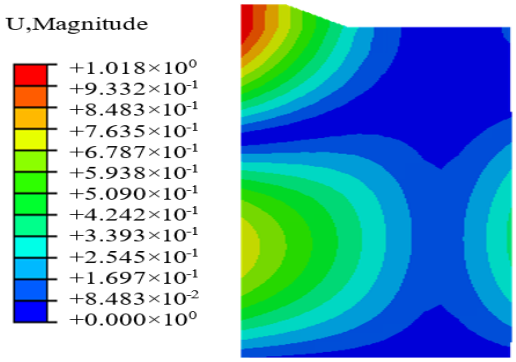

(d) Fourth-order mode

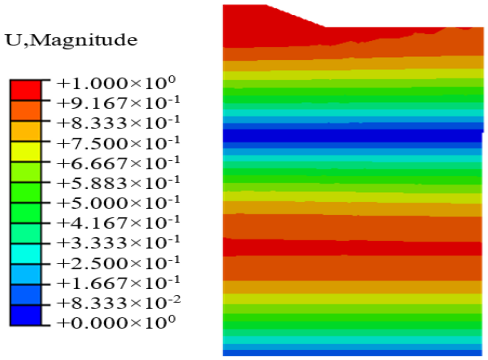

(e) Fifth-order mode

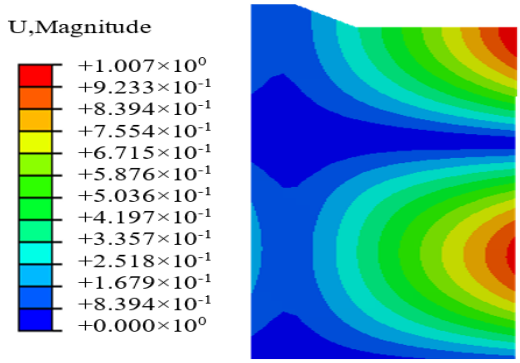

(f) Sixth-order mode

Fig. 5 Vibration pattern of composite foundation

stress boundary and displacement boundary are applied at the same position of the model.

The above three methods of applying train load have their own characteristics. There are similarities between the moving static load method and the artificial excitation method: both can use the solved periodic train load to

Table 3 The first 6 modes of the composite foundation

Mode	1	2	3	4	5	6
Frequency	1. 87	2. 56	3. 74	4. 58	6. 02	7. 33

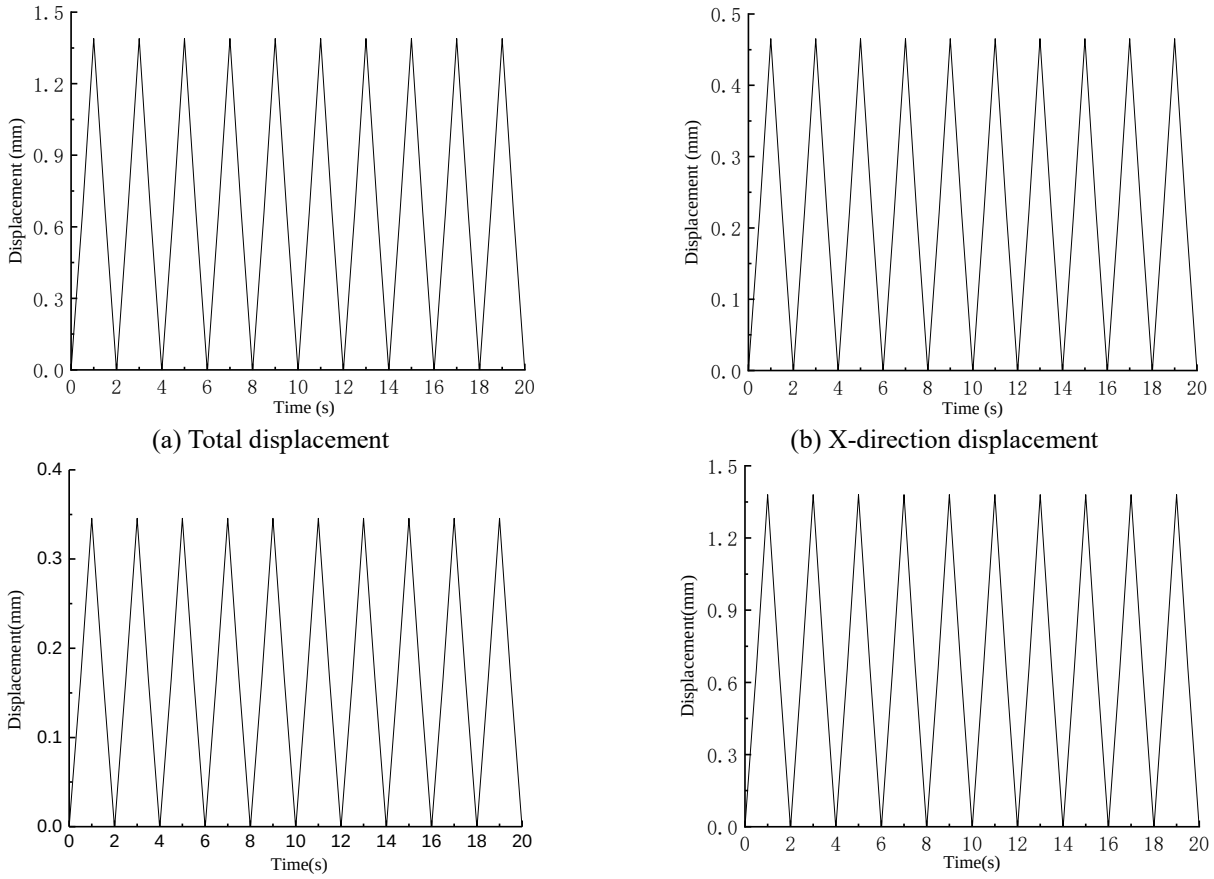

(a) Total displacement (b) X-direction displacement

(c) Y-direction displacement (d) Z-direction displacement

Fig. 6 Time history curve of foundation displacement under train load

simulate the load conditions at different speeds, and both are more used in theoretical establishment or speed-raising analysis. The difference between the two is that the train will produce multi-directional random vibration caused by track surface irregularity, wheel eccentricity, track surface irregularity and wheel spacing in actual operation, and these random vibration factors are not considered in the moving static load method. However, the artificial excitation method considers these random vibration factors to simulate the random vibration in the actual situation, but this method is not very complete to consider the random vibration factors. The advantage of time-history boundary method is that it can better reflect the multi-direction random vibration of the train based on the actual measurement, and through the analysis of the test data, it can accurately predict the response of the subgrade section and other locations around it. The disadvantage is that it cannot directly obtain the load information without monitoring points.

Due to the limitation of conditions, this paper cannot obtain the measured parameters of train load, but the moving static load method does not consider the random factors that will affect the train. After comprehensive comparison (Niu *et al*. 2018), the train load is applied by artificial excitation. In the selection of train axle load, considering the current commonly used high-speed train axle load range is 17 ~ 21t, this paper intends to choose 20t train axle load. The spring mass M_0=750 kg was selected, and the train speed was 300 km/h. From Table 1, the corresponding typical wavelengths and typical vector heights were L_1=10 m, L_2=2 m, L_3=0.5 m, a_1=3.5 mm, a_2=0.4 mm, and a_3=0.08 mm. Based on the above parameters, the time-history curve of train load in the first 20s is drawn by MATLAB software, as shown in Fig. 4.

2.2.3 Dynamic response of composite foundation

In order to study the dynamic characteristics of CFG and cement-soil compaction pile composite foundation, the modal analysis is carried out. The modal analysis step is set to the modal analysis step, and the other analysis steps are suppressed to extract the first six modes of composite foundation. The first six modes displacement nephogram of CFG and cement-soil compaction pile composite foundation is shown in Fig. 5.

The first six natural frequencies of the CFG and cement-soil compaction pile composite foundation are shown in Table 3.

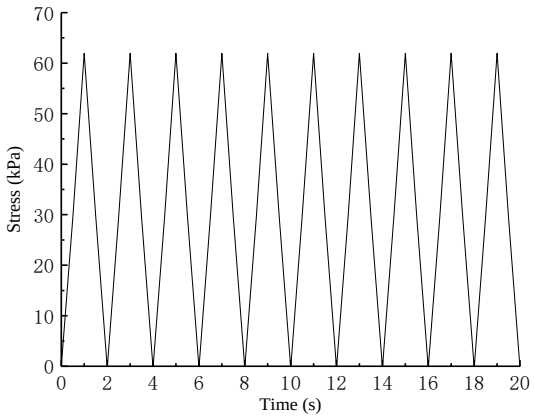

Fig. 7 Stress time history curve

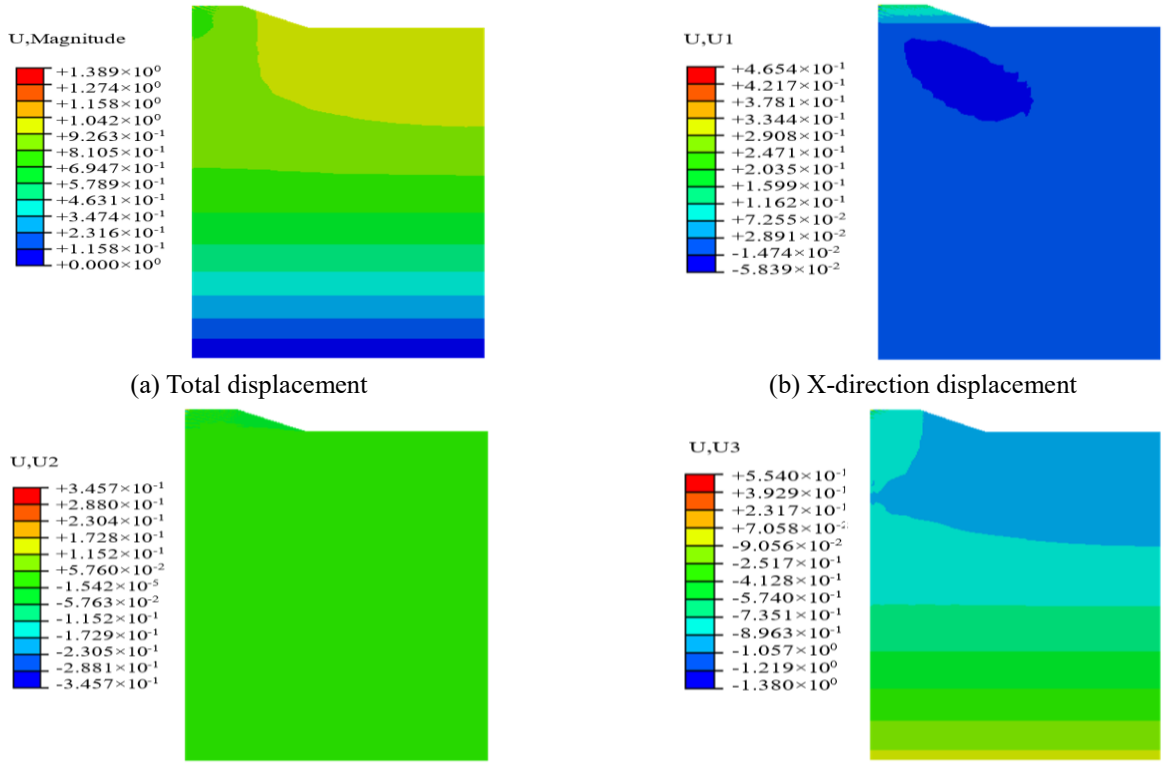

(a) Total displacement (b) X-direction displacement

(c) Y-direction displacement (d) Z-direction displacement

Fig. 8 Displacement nephogram

To study the displacement of CFG and cement-soil compaction pile composite foundation under train load, the train load is applied on the top of the embankment. Since the boundary condition of sides can have a profound impact on results, particularly in the equivalent linear study where the point of interest should be at a reasonable distance from the side boundaries (Naeini and Akhtarpour 2018), so the nodes at the center of the embankment on the symmetric plane of the composite foundation is selected, it is far away from the side boundaries. The displacement time history curve in 20s under train load is extracted, as shown in Fig. 6.

It can be seen from Fig. 6 that the total displacement of the composite foundation, the displacement along X-direction, the displacement along Y-direction and the displacement along Z-direction are roughly harmonically changed with the applied train load. The maximum total displacement is 1.389 mm, the maximum displacement along X-direction is 0.465 mm, the maximum displacement along Y-direction is 0.346 mm, and the maximum displacement along Z-direction is 1.380 mm. Under the train load, the displacement of the composite foundation along the Z-direction is larger than that in the X-direction and Y-direction. This is because the vertical load of the train increases the displacement of the composite foundation along the Z-direction, so the displacement of the composite foundation in the Z-direction is greater than that in the X-direction and Y-direction. It can be seemed that the foundation displacement changing law under train load is similar to the case of Cheng *et al.* (2020).

To analyze the stress state of the composite foundation under the train load, the node at the center of the embankment on the symmetrical surface of composite foundation is selected to extract the stress time-history curve of the composite foundation in 20s under train load, as shown in Fig. 7.

From Fig. 7, it can be seen that under the action of the train load, the stress of the composite foundation at the top of the subgrade changes in a simple harmonic shape, and the peak stress is approximately the same. Because the analysis only considers the effect of the train load and does not consider other external loads, the stress time history curve intuitively reflects the stress variation of composite foundation with the train load.

The time-history curves of displacement and stress at the center of the top surface of the embankment only reflect the changes of displacement and stress at this point with the train load. In order to see the displacement and stress distribution of the whole roadbed more clearly, the displacement nephogram at the time of the maximum displacement is extracted, as shown in Fig. 8.

From Fig. 8, it can be seen that the total displacement of CFG and cement-soil compaction pile composite foundation is 1.389 mm at the maximum displacement moment, which decreases gradually from the top to the bottom of the embankment, and decreases to zero at the bottom of the model. The displacement of the composite foundation along the x-direction decreases gradually from the top of the embankment to the bottom of the subgrade, the maximum value is 0.4654 mm, and the influence on the lower part of the subgrade is small. The displacement of the composite foundation along the y direction is small, and the settlement of the composite foundation in the y-direction is little affected, and the overall change is not large. The maximum displacement of the composite foundation along the z direction is at the train load position on the top of the embankment, and the maximum value is 1.380 mm. The displacement decreases gradually from the top of the embankment to the bottom of the embankment. Through the displacement nephogram, it can be seen that under the action of train load, at the time of maximum displacement, the displacement of composite foundation along the z-direction is the largest, but the displacement amplitude is small, which will not have a significant impact on the normal operation of the train.

The train load will not only affect the displacement of composite foundation, but also affect the stress of composite foundation. In order to study the stress distribution at the maximum stress moment of composite foundation, the finite element analysis results of CFG and cement-soil compaction pile composite foundation under train load are extracted. Because the stress of composite foundation changes periodically with the change of train load, so the nephogram map of each stress peak moment is the same. Taking the stress nephogram map of the first second as an example, the stress analysis of CFG and cement-soil compaction pile composite foundation is carried out. The stress nephogram map of CFG-cement soil compaction pile composite foundation at the maximum stress moment is shown in Fig. 9.

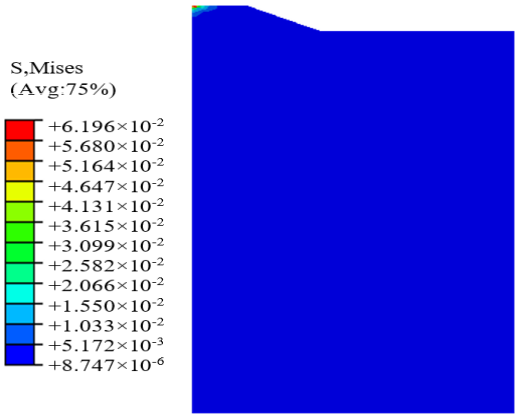

Fig. 9 Stress nephogram

As seen in Fig. 9, at the moment of the maximum displacement, the maximum stress of the composite foundation is the place where the train load is applied, and the maximum value is 61.96 kPa, which decreases gradually downward to a very small value.

The above analysis shows that under the train load, the displacement of CFG and cement-soil compaction pile composite foundation along z-direction is larger, and the displacement along x direction and y direction is smaller. The stress of composite foundation is the largest at the top of embankment, but the displacement and stress values are small, which will not have a great impact on the normal operation of trains. Therefore, the design of CFG and cement-soil compaction pile composite foundation is reasonable.

In practice, earthquakes will also have a great impact on the construction and safe operation of high-speed railway subgrades. It is extremely prone to collapse and other hazards, affecting the normal use of engineering and trains. Therefore, in the next section, the in-depth analysis of the dynamic response of the CFG and cement-soil compaction pile composite foundation under earthquake action is conducted.

3. Dynamic response of CFG and cement-soil compaction pile composite foundation under seismic action

When the Earth's tectonic plates move, they collide and squeeze each other, which can lead to the rapid release of energy, resulting in the vibration of the Earth's crust. The generated energy is transmitted outward in the form of waves. Throughout the ages, earthquakes have brought countless disasters to people's production and lives, including the destruction of houses and casualties. Moreover, earthquakes often bring about many secondary disasters, such as landslides, mudslides, tsunamis, and floods. The occurrence of earthquakes cannot be controlled artificially. At the present level of theoretical research and technology, the occurrence of earthquakes is still unpredictable, and their impacts can only be reduced by means of prevention. Therefore, in construction projects, the seismic design of building structures is indispensable.

3.1 Seismic wave

A seismic wave is a type of elastic wave, which is mainly divided into shear waves, longitudinal waves and surface waves. It is necessary to input the time history curve of the seismic wave acceleration for the dynamic analysis of structures under seismic action. When choosing a seismic wave, three factors of the ground motion should be considered, that is, the spectrum characteristics, peak value and ground motion duration. It is very difficult to select a seismic wave that is completely consistent with the seismic wave of the structure. Therefore, it is necessary to adjust the seismic wave to a more similar structure to obtain more accurate results. The following is a brief introduction to the characteristics of these three elements (Chen *et al*. 2013):

(1) Peak value of acceleration

The selected peak value of the acceleration with the seismic wave should correspond to the peak value of the acceleration required by the local seismic fortification intensity. If not, it should be adjusted according to Eq. (7).

$$a^{'}(t)=\frac{A_{\max}^{'}}{A}a(t) \tag{7}$$

In the formula, $a'(t)$ is the adjusted seismic acceleration curve and A_{max} is the adjusted peak value of the seismic acceleration, taking the peak value of frequent earthquakes and rare earthquakes required by the fortification intensity. $a(t)$ is the original seismic acceleration curve, and A_{max} is the original peak value of the seismic acceleration.

(2) Spectrum characteristics

A spectrum is a description of the frequency components of the ground motion and their degrees of influence. It includes the spectrum shape, peak value, remarkable period and other parameters. The suddenness and randomness of a seismic wave determine its unpredictability, but this does not mean that the seismic wave cannot be addressed mathematically. Since the waveform is difficult to predict, it can begin from the site and select the seismic record according to the characteristics of the site so that the actual seismic record is similar to a seismic pattern that may occur in the future. The seismic spectrum characteristic research shows that the seismic acceleration response spectrum is related to the epicentral distance and the seismic wave period, so when choosing the seismic record, seismic record of the predominant period should be as similar as possible to the actual engineering site characteristics, and the seismic record epicentral distance should also be as close as possible to that of the actual engineering sites.

(3) Ground motion duration

The duration of the seismic wave affects the damage degree caused to ground structures. When determining the duration of a seismic wave, the following principles can be used for reference: the selected duration of the seismic wave should include the strongest part of the seismic record. If only the maximum seismic response analysis at the elastic stage is carried out, then the duration of the seismic wave can be relatively short. If a maximum seismic response analysis at the elastic-plastic stage is needed or if the energy dissipation process of the seismic waves is analyzed, then the duration can be relatively long. Under normal circumstances, the seismic wave duration can be several multiples of the basic period of the structure, and 5 to 10 times is often appropriate.

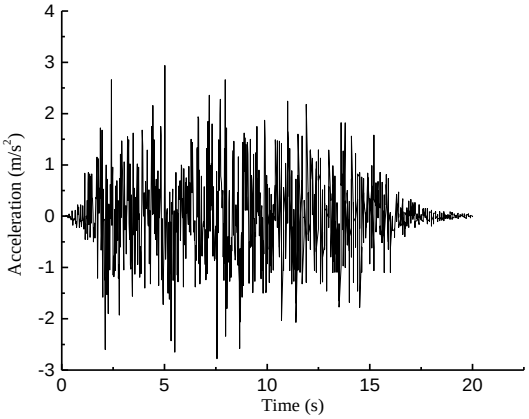

Fig. 10 Lanzhou's wave acceleration time history curve

The time-history analysis method is adopted to analyze the seismic response of the structure through the acceleration time history of the input seismic wave. Since Tianshui city is located in the Lanzhou-Tianshui seismic belt, the Lanzhou wave was selected for the simulation analysis in the seismic response research. According to the Code for Seismic Design of Buildings (GB 50011-2010), the peak seismic acceleration used in the time history analysis of the wheat plot area where the Tianshui South railway station is located should be adjusted to 0.3g (3m/s^2) according to the 8-degree fortification intensity. The time history curve of seismic acceleration after amplitude modulation of Lanzhou wave is shown in Fig. 10.

3.2 Dynamic response of the CFG and cement-soil compacted pile composite foundation

The seismic response of a structure is a nonlinear problem. Although the nonlinear analysis is theoretically more advantageous, the parameters are difficult to determine accurately, the calculation is time-consuming, and the calculation efficiency is low. The nonlinear analysis is thus often only used in a one-dimensional field reaction analysis. From previous study, two main components of the model are the variation in damping ratio and shear modulus reduction with shear strain, it is found that when the damping ratio increase and shear modulus reduction reduce, the shear strain will continue to increase, it shows "parabolic" (Naeini and Akhtarpour, 2018). Although this method can reflect the reality better and accurately, its calculation parameters are not easy to obtain. In order to improve calculation efficiency, in this paper, the equivalent linear calculation is performed by iterative means.

The dynamic solution method of the finite element analysis includes a modal analysis method and direct integration method. The modal analysis method is suitable for linear problems. The direct integration method is suitable for solving nonlinear problems and can be divided

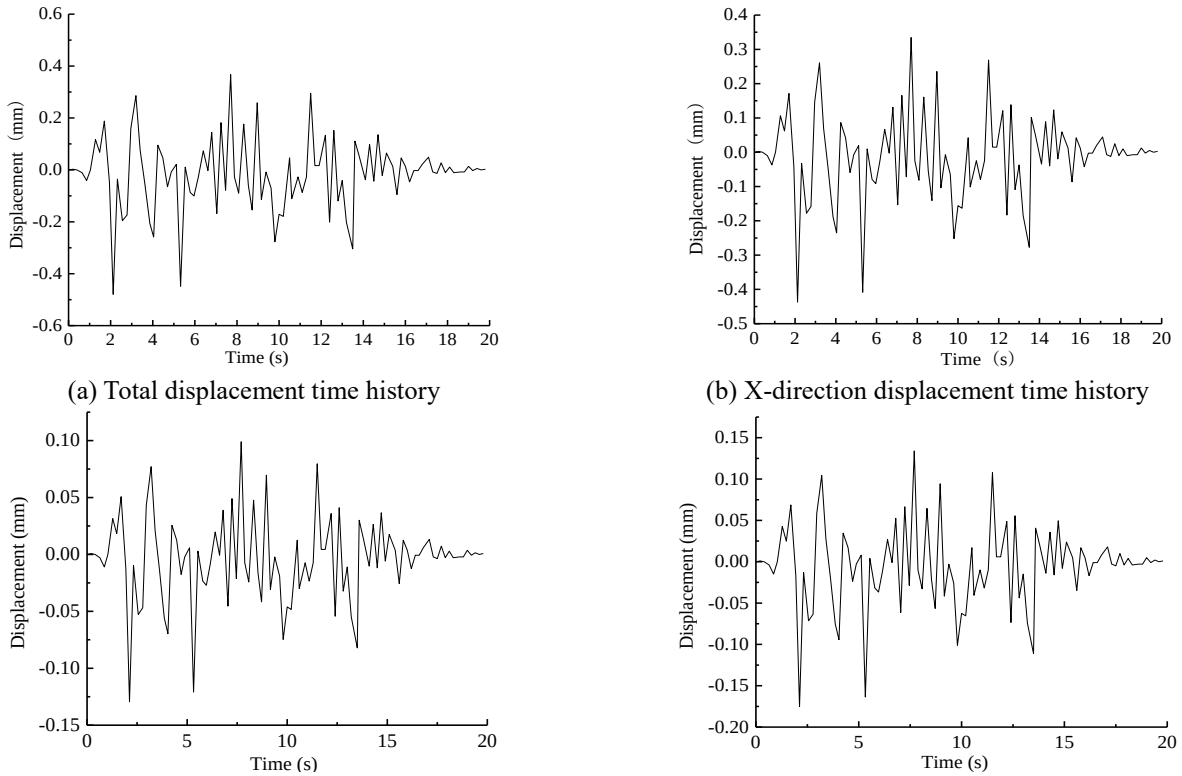

(a) Total displacement time history (b) X-direction displacement time history

(c) Y-direction displacement time history (d) Z-direction displacement time history

Fig. 11 Displacement time history curve

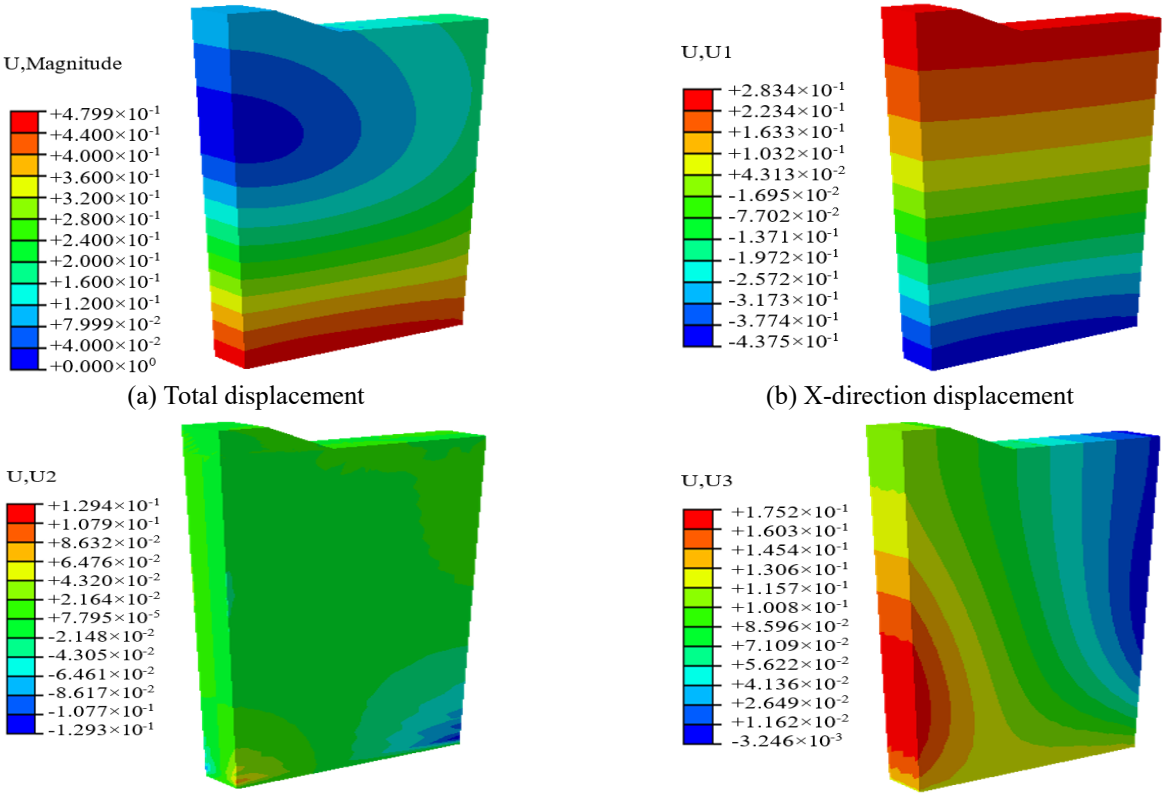

(a) Total displacement (b) X-direction displacement

(c) Y-direction displacement (d) Z-direction displacement

Fig. 12 Displacement nephogram

into the implicit integration method and explicit integration method. Since the display integration method adopts the midpoint interpolation method, there is no need to jointly solve the equations or to solve the tangent stiffness matrix.

Thus, the amount of calculation is smaller than that using the implicit integration algorithm based on the Newton iterative algorithm, and the required calculation space is also small.

Seismic waves are a type of dynamic load that is selected during the loading process. First, the adjusted seismic wave is introduced into the amplitude curve. When the boundary condition is set, the Z-direction displacement at the bottom of the model is fixed, and the horizontal seismic wave is applied from the ground base as a boundary condition. The constraint type is selected as the acceleration, the shear wave in the X-direction is input at the bottom of the model, and the magnitude of the amplitude is selected as the imported seismic wave.

To study the displacement and stress of the CFG and cement-soil compacted pile composite foundation under the influence of seismic action, the Lanzhou seismic wave with a time duration of 20 s is input at the base of the road, and finite element analysis is carried out to select the top surface of the embankment. The node at the center point of the symmetry plane extracts the displacement time history curve in the analysis result, as shown in Fig. 11.

Fig. 11 shows that the ground displacement is consistent with the seismic fluctuation trend under seismic action. The total displacement peak value is 0.4799mm, the X-direction displacement peak value is 0.4375mm, the Y-direction displacement peak value is 0.1294mm, and the Z-direction displacement peak value is 0.1752mm.

The displacement and stress time history curves at the node in the center of the top surface of the embankment only reflects the changes in the displacement and stress with the seismic wave. To see the displacement and stress distributions of the entire embankment more clearly, the displacement nephograms of the maximum displacement moment around the composite foundation are extracted from the analysis results, as shown in Fig. 12.

It can be seen in Fig. 12 that under the action of a seismic wave, the maximum displacement of the composite foundation at the moment of maximum displacement is 0.4799mm, which is located at the bottom of subgrade, where the seismic wave input is located. The maximum displacement along the X-direction is 0.4375mm, which is also at the bottom of the model, and it gradually decreases upward until the direction changes near the lower embankment. The overall displacement along the Y-direction is small; it is the largest at the bottom of the model, with a maximum value of 0.1294mm, and gradually decreases upward. The displacement along the Z-direction varies greatly in the horizontal direction of the embankment and has a maximum value of 0.1752mm. It is located at the center of the embankment at the bottom of the model and decreases upward. The displacement direction changes near the foot of the embankment slope and tends to increase towards the outer edge. It can be concluded that the foundation displacement is very small under seismic action, similar to the case of Ding *et al.* (2008; 2015).

Earthquakes affect not only the displacement of the composite foundations but also the stress conditions. To study the stress variation of the composite foundation under the action of a seismic load, a stress time history analysis of the composite foundation is carried out. The analysis results are shown in Fig. 13.

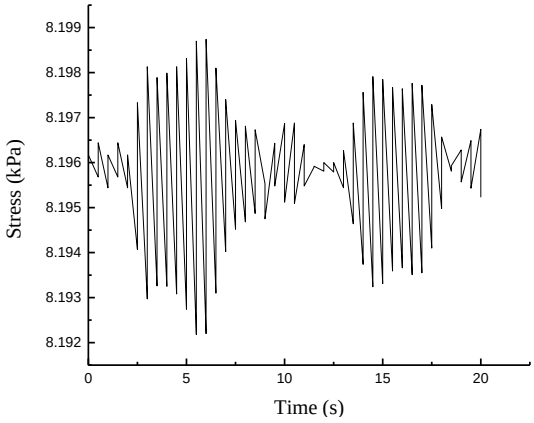

Fig. 13 Stress time history curve

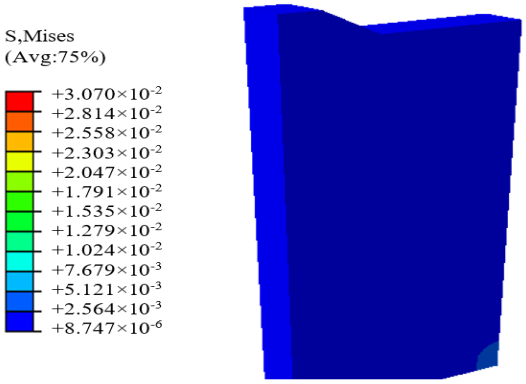

Fig. 14 Cloud moment of maximum stress

From Fig. 13, it can be seen that the trend of the stress-time history curve is similar to that of the seismic wave, reaching a maximum at 7.6 s and a minimum at 10 s. The maximum stress of the composite foundation under seismic action is 8.199 kPa, and the minimum is 8.192 kPa. It can be seen that the stress on the top of the composite foundation is small and the range of change is small; thus, it will not have a great impact on the train operation.

To study the stress distribution of a composite foundation at the moment of maximum stress, the finite element analysis results are extracted. Because the stress of the composite foundation varies with the magnitude of the seismic action, a stress analysis of the CFG and cement-soil compaction pile composite foundation can be carried out. The stress nephogram of the composite foundation is shown in Fig. 14.

In Fig. 14, under the action of a seismic wave, the maximum stress value at the moment is 30.70kPa, located at the bottom of the model seismic wave input, and gradually decreases toward the upper part of the model to a minimum value of 5.97×10^{-3}kPa at the top of the model. It is known that under the seismic action, the surface stress of the embankment is very little affected.

According to the above analysis, under seismic action, the displacement and stress of a composite foundation are larger at the bottom, while that of the embankment is very small, which will not have an impact on the normal operation of the train.

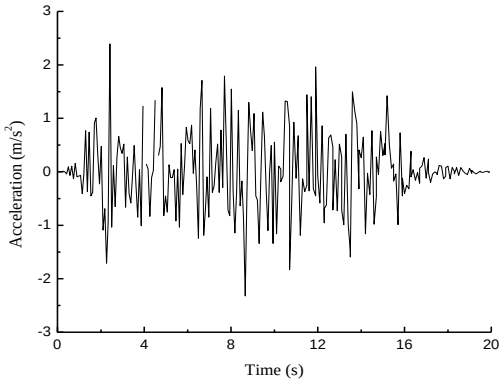

Fig. 15 Acceleration time history curve

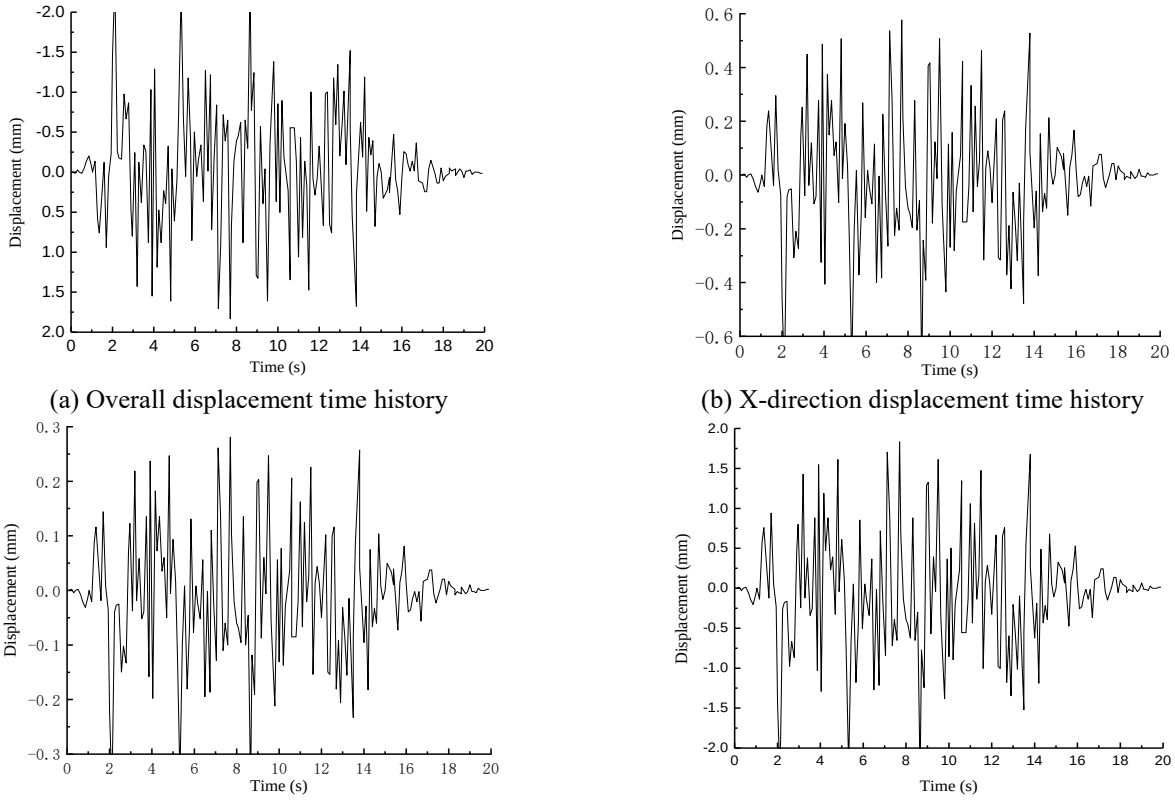

(a) Overall displacement time history

(b) X-direction displacement time history

(c) Y-direction displacement time history

(d) Z-direction displacement time history

Fig. 16 Time history curve of foundation displacement under train-seismic

3.3 Dynamic response of CFG and cement-soil compaction pile composite foundation under train-seismic action

It can be seen from the previous analysis of Section 2.2 and Section 3.2, which show that the influences of the train load and seismic action on the composite foundation alone are not large; however, since there is a possibility of the composite foundation being acted upon simultaneously by both a train and a seismic wave in practical engineering, this section intends to study the dynamic response of a train-seismic load in a railway operation stage. Therefore, in this section, the dynamic response of CFG and cement-soil compaction pile composite foundation under train-seismic load is studied. The acceleration time curve of the CFG and cement-soil compaction pile composite foundation under train-seismic action is shown in Fig. 15.

It can be seen in Fig. 15, the acceleration of the composite foundation shows a certain fluctuation, which is consistent with the variation trend of the input seismic wave in Lanzhou, but the amplitude of the acceleration is smaller than that of the input seismic wave, which is due to the damping effect of the foundation soil, so the acceleration decreases.

To study the displacement of the CFG and cement-soil compacted pile composite foundation under the combined action of the train load and seismic wave, a 20s vertical train excitation was applied on the top surface of the embankment and 20s horizontal seismic waves were input into the bottom of the embankment to conduct a finite element analysis of the model. In the analysis results, the node at the center of the top surface of the embankment was

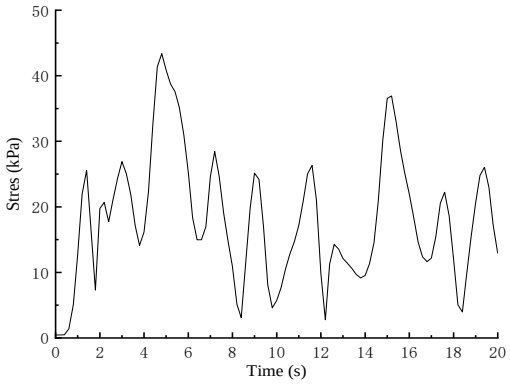

Fig. 17 Time-course curve of foundation stress under train-seismic load

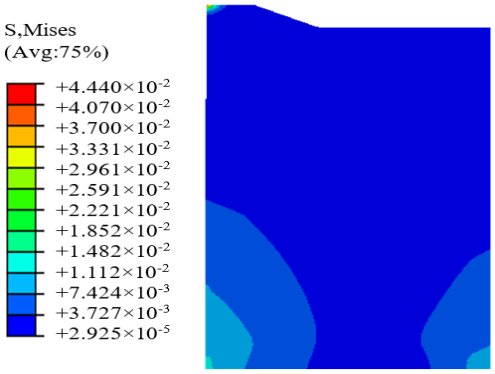

Fig. 18 Stress nephogram

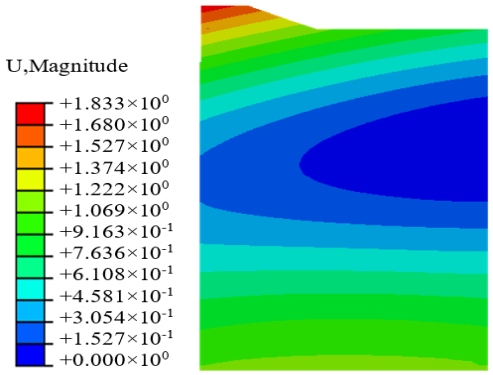

(a) Total displacement

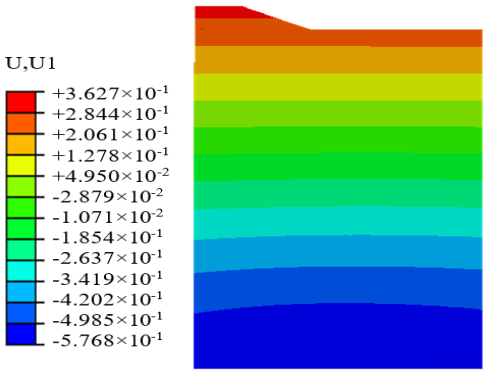

(b) X-direction displacement

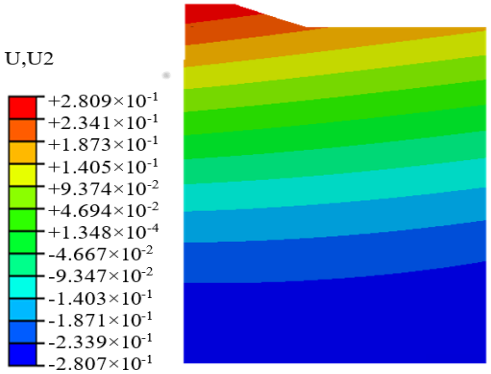

(c) Y-direction displacement

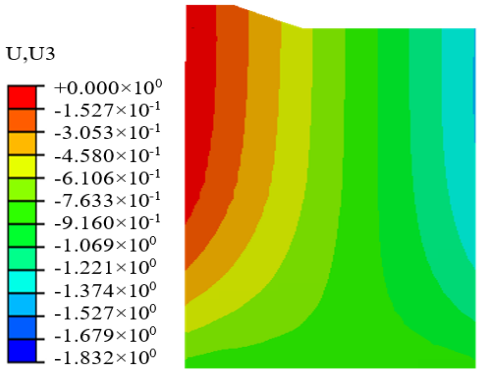

(d) Z-direction displacement

Fig. 19 Displacement nephogram of composite foundation at maximum displacement

selected to extract the displacement time-history curve of the composite foundation within 20s under the combined action of the train and the seismic wave, as shown in Fig. 16.

Fig. 16 shows that under the combined action of seismic and train loads, the displacement reaches its peak at 9 s, and the maximum total displacement of the composite foundation is 1.833 mm, which is consistent with the variation trend of the applied load. The maximum displacement along the X-direction is 0.567 mm. The change trend of the displacement along the Y-direction is similar to that of the total displacement, with the maximum displacement being 0.281 mm, and the maximum displacement is 1.832 mm along the Z-direction. Under the combined action of seismic and train loads, the total displacement, displacement along the X-direction, displacement along the Y-direction and displacement along the Z-direction of the composite foundation are larger than those under the separate actions of the train load or seismic load, but the ranges of increase are smaller.

To study the variation of the stress of the composite foundation with time under a train-seismic load, a stress time-history analysis was carried out for the composite foundation. The finite element analysis results are shown in Fig. 17.

Fig. 17 shows that the stress variation trend of the composite foundation under train-seismic action is that the stress of the composite foundation fluctuates to a certain extent, but the stress is small, and thus it will not have a great impact on the normal operation of the composite foundation.

The displacement and stress time history curves of the node at the center of the top surface of the embankment only reflect the changes in displacement and stress at the point with the train-seismic load. To see the displacement and stress distributions of the entire embankment more clearly, the maximum dynamic response of the foundation is analyzed and the stress nephogram at the maximum stress moment is extracted, as shown in Fig. 18.

From Fig. 18, it can be seen that the stress reaches the maximum value at the both sides edges of the bottom of the model and decreases gradually towards the inside and the top. The stress at the place where the train load is applied is also larger and decreases moving downward.

To study the displacement distribution of the CFG and cement-soil compaction pile composite foundation under the combined action of train and seismic loads, it is necessary to extract the displacement nephograms of the composite foundation, which are shown in Fig. 19.

Fig. 19 shows that at the moment of the maximum displacement, because the train load is applied at the top of the model and the seismic waves are input at the bottom, the displacements at the top and bottom of the model are larger and that at the middle is smaller. The displacement along the X-direction is the largest at the bottom of the model, with a value of 0.5768mm, and gradually decreases towards the top of the model. It can be seen that in the horizontal direction, the seismic waves have a greater impact. At the moment of the maximum displacement, the composite foundation has the maximum displacement at the top of the embankment, with a maximum value of 1.833mm, and it decreases gradually towards the bottom of the model. The displacement at the middle part of the model is the minimum, and the displacement at the bottom is the same as that at the top of the embankment, and it decreases gradually towards the top of the model. This is because the upper train load has a greater impact on the displacement, while near the bottom, the seismic load has a greater impact. The maximum displacement along the Y-direction is 0.2807 mm, and the change trend is opposite to that along the X-direction. At the top of the model, the displacement decreases towards the bottom of the CFG pile. The displacement at the bottom is slightly smaller than that at the top of the embankment, but in the opposite direction, it gradually decreases towards the top of the model. The displacement along the Z-direction is the largest at the top of the embankment, with a maximum value of 1.832mm, and it decreases gradually around the embankment. The displacement direction near the foot of the embankment slope changes, and its value increases gradually towards the edge of the model. This is because the train load directly acts on the embankment surface and thus has a greater impact on it. However, far from the embankment, the influence of the train load decreases, and the effect of the seismic load is more obvious.

4. Conclusions

- Under the action of train load, the maximum settlement of the composite foundation is 1.389 mm at the action of the train load, and it gradually decreases towards the bottom of the embankment. However, the overall displacement is small and thus has little impact on train operation.
- Under the action of a seismic load, the maximum settlement of the composite foundation is 0.4799 mm. When affected by seismic waves, the displacement is the largest at the bottom of the embankment and gradually decreases towards the top of the embankment, and so it has little impact on the top of the embankment.
- Under the train-seismic action, the maximum settlement of the composite foundation is 1.833 mm. The displacements at the bottom of the subgrade and the top of the embankment are large and gradually decrease towards the middle.

The main influence area of the train load and seismic action on the settlement of the composite foundation is at the action position of the load, but the influence is not great. Under the action of the train load, the seismic load and train-seismic loads, the settlement of the roadbed is small, and thus, the operation of the train will not be greatly affected.

Acknowledgments

This paper was funded in part by the National Natural Science Foundation of China (51968045), and a part of science and technology project in China Railway 21th Bureau Group (Grant number: 14B-3), and a part of science and technology project in China Railway Construction Corporation Limited (Grant number: 17-C21).

References

Cheng, X.S. and Jing, W. (2017), “Settlement analysis of saturated tailings dam treated by CFG pile composite foundation”,

Geomech. *Eng*., **13**(6), 929-946. https://doi.org/10.12989/gae.2017.13.6.929.

Cheng, X., Liu, G., Gong, L., Zhou, X. and Shi, B. (2020), "Mechanical characteristics+ differential settlement of CFG pile and cement-soil compacted pile about composite foundation under train load", *Geomech*. *Eng*., **20**(2), 155-164. https://doi.org/10.12989/gae.2020.20.2.155.

Castro, J. and Sagaseta, C. (2009), "Consolidation around stone columns: Influence of column deformation", *Int*. *J*. *Numer*. *Anal*. *Met*. *Geomech*., **33**(7), 851-877. https://doi.org/10.1002/nag.745.

Ding, J.H., Liu, F.R. and Du, E.X. (2008), "Dynamic characteristic analysis on composite foundation with soil-cement piles and CFG piles", *Fly Ash Comprehens*. *Utiliz*., (6), 37-40.

Ding J.H., Feng J.H., Zhang P.X. and Quan, X.Z. (2015), "Experimental study on dynamic characteristics of composite foundations of rammed cement-soil loop piles with CFG cores", *Eng*. *Mech*., **32**(S1), 284-288. https://doi.org/10.6052/j.issn.1000-4750.2014.05.S041.

Faro, V.P., Consoli, N.C., Schnaid, F., Thomé, A. and Lopes, L.S. (2015) "Field tests on laterally loaded rigid piles in cement treated soils", *J*. *Geotech*. *Geoenviron*. *Eng*., **141**(6), 06015003.1-06015003.7. https://doi.org/10.1061/(ASCE)GT.1943-5606.0001296.

Germonpré, M., Nielsen, J.C.O., Degrande, G., Lombaert, G. (2018). "Constributions of longitudinal track unevenness and track stiffness variation to railway induced vibration", *J*. *Sound Vib*., **437**(2018), 292-307. https://doi.org/10.1016/j.jsv.2018.08.060.

Handy, R.L. (2001), "Does lateral stress really influence settlement", *J*. *Geotech*. *Geoenviron*. *Eng*., **127**(7), 623-626. https://doi.org/10.1061/(ASCE)1090-0241(2001)127:7(623).

Lai, J.X., Liu, H.Q., Qiu, J.L. and Chen, J.X. (2016) "Settlement analysis of saturated tailings dam treated by CFG pile composite foundation", *Adv*. *Mater*. *Sci*. *Eng*., 1-10. https://doi.org/10.1155/2016/7383762.

Loganathan, N., Balasubramaniam, A.S. and Bergado, D.T. (1993), "Deformation analysis of embankments", *J*. *Geotech*. *Eng*., **119**(8), 1185-1206. https://doi.org/10.1061/(ASCE)0733-9410(1993)119:8(1185).

Leung, Y.F., Klar, A., Soga, K. and Hoult, N.A. (2017), "Superstructure-foundation interaction in multi-objective pile group optimization considering settlement response", *Can*. *Geotech*. *J*., **54**(10), 1408-1420. https://doi.org/10.1139/cgj-2016-0498.

Milnen, D.R.M., Le Pen, L.M., Thompson, D.J. and Powrie W. (2017), "Properties of train load frequencies and their applications", *J*. *Sound Vib*., **397**, 123-140. http://doi.org/10.1016/j.jsv.2017.03.006.

Moayed, R.Z., Izadi, E. and Mirsepahi, M. (2013), "3D finite elements analysis of vertically loaded composite piled raft", *J*. *Cent*. *South Univ*., **20**(6), 1713-1723. http://doi.org/10.1007/s11771-013-1664-y.

Nie, R.S., Tang, S.M., Leng, W.M., Yang, Q. and Cheng, L.H. (2017), "Field measurement of high-speed train-induced vertical loads on bridge pile foundations", *J*. *China Railway Soc*., **39**(9), 148-154. http://doi.org/10.3969/j.issn.1001-8360.2017.09.021.

Niu, T.T, Liu, H.L., Ding, X.M. and Chen, Y.M. (2018), "Piled embankment model test on vibration characteristics under high-speed train loads", *Rock Soil Mech*., **39**(3), 872-880. http://doi.org/10.16285/j.rsm.2016.0680.

Naeini, M. and Akhtarpour, A. (2018). "Numerical analysis of seismic stability of a high centerline tailings dam", *Soil Dyn*. *Earthq*. *Eng*., **107**, 179-194. http://doi.org/10.1016/j.soildyn.2018.01.0193.

Sales, M.M., Prezzi, M., Salgado, R., Choi, Y.S. and Lee, J. (2017), "Load-settlement behaviour of model pile groups in sand under vertical load", *J*. *Civ*. *Eng*. *Manage*., **23**(8), 1148-1163. https://doi.org/10.3846/13923730.2017.1396559.

Smadi, M.M. (2001), *Lateral Deformation and Associated Settlement Resulting from Embankment Loading of Soft Clay and Silt Deposits*, University of Illinois at Urbana–Champaign, Urbana, U.S.A.

Sun, X. J., Yuan, Y., Ma, M. and Liu, W.N. (2017), "Prediction of metro train-induced low frequency vibration responses in far field", *J*. *Vib*. *Shock*, **36**(4), 198-202. https://doi.org/10.13465/j.cnki.jvs.2017.04.031.

Wang, C.D., Zhou, S.H., Wang, B.L. and Guo, P.J. (2018), "Time effect of pile-soil-geogrid-cushion interaction of rigid pile composite foundations under high-speed railway embankments", *Geomech*. *Eng*., **16**(6), 589-597. https://doi.org/10.12989/gae.2018.16.6.589.

Xue, S.S., Chen, Y.M. and Liu, H.L. (2019), "Model test study on the influence of train speed on the dynamic response of an X-section pile-net composite foundation", *Shock Vib*., 1-13. https://doi.org/10.1155/2019/2614709.

Zhang, Y.E. and Bai, B.H. (2001), "Study on the vibration response of tunnel subjected to high speed train loading", *J*. *Vib*. *Shock*, **20**(3), 93-95. https://doi.org/10.13465/j.cnki.jvs.2001.03.028.

Zhang, Z.T., Gao, W.H., Wang, X., Zhang, J.Q. and Tang, X.Y. (2020), "Degradation-induced evolution of particle roundness and its effect on the shear behaviour of railway ballast", *Transport*. *Geotech*., **24**, 100388. https://doi.org/10.1016/j.trgeo.2020.100388.

Zhang, Z.T. and Gao, W.H. (2020), "Effect of different test methods on the disintegration behaviour of soft rock and the evolution model of disintegration breakage under cyclic wetting and drying", *Eng*. *Geol*., **279**, 105888. https://doi.org/10.1016/j.enggeo.2020.105888.

CC